PERGAMON

Solid State Communications 124 (2002) 363–371

solid state communications

www.elsevier.com/locate/ssc

Research Paper

An ultrasound emitter based on assisted tunneling

L.E.F. Foa Torres[a], H.M. Pastawski[a,*], S.S. Makler[b,c]

[a]*Facultad de Matemática, Astronomía y Física, Universidad Nacional de Córdoba, Ciudad Universitaria, 5000 Córdoba, Argentina*
[b]*Instituto de Física, Universidade Federal Fluminense, Niterói, RJ, Brazil*
[c]*Instituto de Física, Universidade do Estado do Rio de Janeiro, RJ, Brazil*

Received 24 May 2002; accepted 2 August 2002 by A. Pinczuk

Abstract

The problem of electron tunneling assisted by an elementary excitation in a double barrier resonant device is usually described within a sequential (decoherent) approximation. By solving exactly the many-body problem for a simplified model of electron–phonon interaction we show, analytically and numerically, that the assisted tunneling peak can be strongly enhanced by an appropriate election of the geometrical parameters of the device. This induces a symmetry condition in the Fock space that maximizes the effectiveness of the scattering process. We propose that this process could provide the primary longitudinal optical phonons required to operate a phonon laser (SASER). © 2002 Elsevier Science Ltd. All rights reserved.

PACS: 73.63.Hs; 73.63.−b; 73.40.Gk; 71.38.−k

Keywords: A. Nanostructures; A. Quantum wells; A. Semiconductors; D. Saser; D. Phonons

1. Introduction

The continuous downscaling of electronic devices from the layered semiconductor heterostructures to nanostructures and more recently, to molecular systems, have been paralleled by a great progress in the understanding and control of electronic transport [1,2]. These advances led to the observation of novel quantum phenomena. Undoubtedly, a key idea behind these advances has been Landauer's view [3,4] of *conductance as a transmittance*, whose conceptual simplicity was instrumental to trigger the innovation. However, the electron–electron (e–e) and the electron–phonon (e–ph) interactions may add substantial complexity to the electronic problem, limiting its application. The e–e interaction can be often addressed in a mean field approach and has received much attention in different contexts such as single electron transistors, electron pumps, turnstiles and interferometers. In contrast, the e–ph interactions lag behind in terms of applications. After the observation of optical phonon-assisted tunneling [5–7] interest on e–ph interaction remained focused in double barrier Resonant Tunneling Devices (RTD) until the recent observation of related electro-mechanical effects in molecular systems [8–10]. Since only the simple qualitative questions related to these phenomena have been addressed, a fresh reconsideration of the problem could lead to substantial progress in an underdeveloped area. In this paper we will perform such conceptual revision with a focus on an extension of the Landauer's view to the e–ph Fock space that will allow the design of a sound emitter.

The careful measurement of the current–voltage (I–V) curve in AlGaAs-GaAs RTDs shows [5–7], besides the usual elastic resonance peak, a weak satellite peak rising in the valley of the I–V curve. This occurs when the energy of an electron in the emitter exceeds the energy of the ground state in the well by just a quantum of the well's longitudinal optical (LO) vibrational mode. This enables the *decay of an electron* with kinetic energy $\varepsilon \leq \varepsilon_F$ and potential energy eV in the emitter *into an electron* with kinetic energy $\varepsilon + eV - \hbar\omega_0$ in the collector *plus a* LO *phonon* (see Fig. 1(a)). By applying a strong magnetic field the satellite peaks become very thin limited only by the electronic lifetimes and the small LO phonon bandwidth lower than 10^{-2} meV $\ll \hbar\omega_0 \simeq 36$ meV. In these RTDs even when the LO phonons are confined to the well, they have a short

* Corresponding author. Fax: +54-351-4334-054.
E-mail address: horacio@famaf.unc.edu.ar (H.M. Pastawski).

PII: S0038-1098(02)00427-1

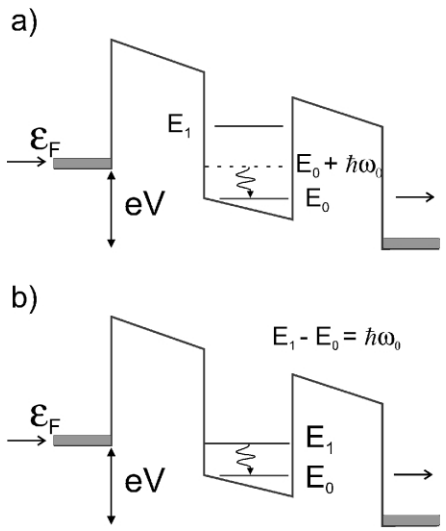

Fig. 1. Schematic representation of the processes leading to the phonon emission for two different RTD configurations. E_0 and E_1 represent the first two electronic levels in the well. In a) only the electronic ground state and the first polaronic state of one electron plus one phonon (depicted as a dotted line) are relevant. In figure b) the device parameters are chosen in order to satisfy the condition: $E_1 - E_0 = \hbar\omega_0$.

lifetime [11] because they decay into a pair of LO and transverse acoustic (TA) phonons. The expectation that the secondary TA phonons can form a coherent beam inspired a proposal for the generation of a coherent **sound** beam (in the region of 2 THz) which justifies the name of **S**ASER in analogy with **L**ASER [12,13] for such device. The critical intensities required for stimulated decay of the primary phonons were recently discussed [14]. Although definitive rates would be those provided by experiments, it is clear that operation in the 'sasing' regime would require an important source of primary optical phonons. The devices considered previously in this context Refs. [13,15] *required* an energy difference between the first two electronic states in the well satisfying the resonant condition $E_1 - E_0 = \hbar\omega_0$ (see Fig. 1(b)). This situation is exactly analogous to that of a LASER. However, while in a LASER there is always a photon mode satisfying such condition, in a SASER the phonon energy is a fixed magnitude. Therefore, the onset of the 'sasing' regime would require the careful construction of a specifically designed device. This task proves particularly difficult as the frequencies of phonon modes and interaction strengths are not easy to predict from the current status of the theory [16]. Therefore, one would desire an alternative design where a resonant condition could be tuned up by an external parameter such as the voltage.

A way to overcome the mentioned difficulties appears when one realizes [17] that an electron trapped in a resonant state dresses itself with vibrational modes that forms a polaron. When the barriers allow tunneling these get a lifetime becoming polaronic resonances whose relative energy can be tuned by the electric field to achieve the phonon emission. The resulting scheme is just that of phonon-assisted tunneling, which is represented in panel a) of Fig. 1. Our new point over the established description of phonon-assisted tunneling emission is that phonon emission could be considerably enhanced by requiring a specific balance between the rates at which these many-body polaronic resonances are build up and decay. Since these rates can be related to the single electron tunneling escape rates through the barriers which in turn depend on the geometry of the barriers, the last can be tailored to enhance significantly the LO phonon emission. A relevant point is that the present proposal does not require an accurate definition of the geometry dependent device parameters. Instead, the operation in the phonon emission mode *only* requires the tuning of the many-body resonance achieved by the applied voltage.

This paper is organized as follows. In Section 2 we give a brief perspective of the main theoretical approaches for phonon assisted tunneling in RTD's. In Section 3 we introduce our model and derive analytical expressions that synthesize the physics presented above. Section 4 is devoted to the presentation and discussion of numerical results. Our conclusions are given in Section 5.

2. Theoretical background

The first solutions of transport in an RTD including strongly inelastic e–ph scattering [18–20] considered a single electron state in the well interacting with optical phonons. The scattering problem was solved, in a one electron approximation, by computing the many-body Green's functions. Its solution requires some simplifications such as imposing energy independent couplings to the electrodes [18] ('broad band' approximation). In this coherent picture, a tight-binding model [21] yields similar results. Further studies went beyond the simplified e–ph interaction to include the full phonon band and electron recoil [22,23]

A conceptually different approach considered the e–ph interaction as a source of decoherence and thermalization for the electrons in a resonant region [24] by adopting a complex self-energy correction [25] to the electronic states. Therefore, in this description, the phonon system acts in a way analogous to the 'voltage probes' in the Büttiker's formulation of Landauer's picture. *Only those electrons that do not interact with phonons maintain coherence* with its source. This line, which finds full formal support within the Keldysh formalism [26,27], has been further developed [16] to include strongly inelastic processes and originated computational codes [28] that simulate mesoscopic devices.

The most frequent scheme is the use of rate

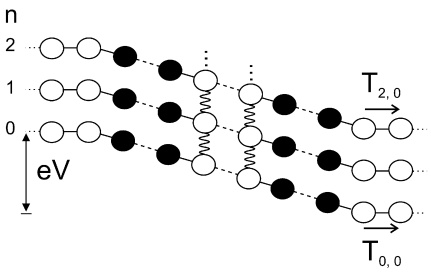

Fig. 2. Representation of the model. Each site is a state in the Fock space: The different rows are states with different number of phonons in the well (n). The sites in black are in the barriers. Straight lines are hoppings and wavy lines are e–ph couplings.

equations [16,29]. The calculation of the rate transition probabilities used in this method relies on the application of the Fermi Golden Rule (FGR) at two stages: a) It describes the tunneling entrance to the well and its ulterior escape independently. There, quantum coherent effects are ignored since it is assumed that the phase of the electronic wave function is randomized by some mechanism. Within this sequential tunneling picture, the electron tunnels into the well and, after losing memory of its phase, it tunnels out of the well. b) Once the electron is inside the well, the phonon emission is also studied with the FGR. These approximations require a weak e–ph coupling with a dense phonon spectrum justifying the FGR and the electronic decoherence.

In this work, we use a fully coherent description of the joint processes of tunneling and phonon emission. This approach, introduced in Refs. [12] and [30], while containing the semiclassical rate equation limit in the appropriate conditions, is able to describe many-body phenomena that are beyond a decoherent description. The general many-body problem can be simplified if one considers a single electron interacting with the phonons. This problem can be exactly mapped into a one-body scattering in a higher dimensional system. Each phonon mode can be seen as a new dimension of an 'electronic' variable. Within this equivalent problem, the transmission probability of electrons between incoming and outgoing channels with different number n of phonons can be calculated exactly from the Schrödinger equation. Its solution is easily obtained by a truncation of the Fock space that only includes states within some range of n. This range can be expanded until the answer converges, allowing a variational, non-perturbative calculation. Thus, we are not restricted to a weak e–ph coupling. It must be emphasized again that in this approach the e–ph interaction is not assumed to produce a phase randomization, as quantum phases are fully conserved. Instead of calculating transition rates, the complex quantum amplitude for each state in the Fock space is obtained.

3. Model and analysis

We want to model the electronic transport through an RTD including the coherent effects of the e–ph interaction in the well region. By assuming translational invariance in the plane perpendicular to the current flow, the equations can be decoupled for each wave-vector $\mathbf{k}_\perp$ in this plane. The resulting Hamiltonian will be the sum of 1-d Hamiltonians for each $\mathbf{k}_\perp$. In what follows, we will first consider the 1-d problem and this index ($\mathbf{k}_\perp$) will be omitted. To this end we will introduce a Hamiltonian that is a sum of an electronic contribution $\mathscr{H}_e$, a phonon contribution $\mathscr{H}_{ph}$ and an electron–phonon interaction term $\mathscr{H}_{e-ph}$

$$\mathscr{H} = \mathscr{H}_e + \mathscr{H}_{ph} + \mathscr{H}_{e-ph}. \tag{1}$$

The electronic part is modeled by means of a single band described by

$$\mathscr{H}_e = \sum_j E_j c_j^+ c_j - \sum_{i,j} V_{i,j}(c_i^+ c_j + c_j^+ c_i), \tag{2}$$

which represents a nearest-neighbor tight-binding Hamiltonian for the electrons, where c_j^+ and c_j are electron operators at site j on a 1-d chain that includes a number of sites in the barriers and the well. The hopping parameters $V_{j,j+1} = V$ are defined in terms of the effective mass m^* and the lattice constant a as $V = \hbar^2/(2m^*a^2)$. The site energies E_j model the potential profile. We assume that the potential energy drop eV is linear through the double barrier and limited to it. The physical dimensions correspond to the situation where there is a single resonant peak in the energy range of interest. N_L and N_R are the number of sites in the left and right barriers and N_W are those in the well, the associated widths are $L_i = N_i a$. In what follows, the widths of the barriers and the well will be expressed in units of this constant.

The most important interaction between electrons and phonons in polar semiconductors involves a longitudinal optical (LO) phonon band $\hbar\omega[\mathbf{q}_\perp, q]$ and is limited to the well region. Even when an electron state can interact with different modes, it was found [22] that the dominating decay process (focusing effect) occurs through the mode with $\mathbf{q}_\perp = \mathbf{k}_\perp$. This justifies to consider only one phonon mode per transversal state. Moreover, the weak dispersion relation of the LO phonons ($\hbar\omega[\mathbf{k}_F, \pi/L_w] - \hbar\omega_0 < 10^{-2}$ meV) leads to the use of a single frequency $\hbar\omega_0 = 36$ meV for all the modes and a single coupling constant denoted by V_g. Then, the phonon and the electron–phonon terms of the Hamiltonian are given by:

$$\mathscr{H}_{ph} = \hbar\omega_0 b^+ b, \tag{3}$$

and

$$\mathscr{H}_{e-ph} = V_g \sum_{j[\text{well}]} c_j^+ c_j (b^+ + b), \tag{4}$$

where b^+ and b are the creation and annihilation operators for phonons. Then, if we consider the Fock space expanded

by $|j,n\rangle = c_j^+(b^+)^n/\sqrt{n!}|0\rangle$, the many-body problem maps to the 2-dimensional one-body problem shown in Fig. 2. The vertical dimension is the number n of phonons [12,30].

Numerical results for the model described by the Hamiltonian of Eqs. (2–4) will be presented in the next section. In order to obtain analytical expressions for the transmittances and currents the model can be further simplified if one considers only the electronic ground state in the well. Therefore, one gets a resonant central site that interacts with the phonons and is weakly coupled to the leads. Then, $E_0 = E_{(o)} - \alpha e\mathrm{V}$ is the well's *ground state* which is shifted by the electric field and $V_{0,1} = V_\mathrm{R}$ and $V_{-1,0} = V_\mathrm{L}$ (notice that $V_{\mathrm{L(R)}} \ll V$) which fix the tunneling rates through the barriers. The site energies are $E_j = 2V$ for $j < 0$ and $2V - e\mathrm{V}$ for $j > 0$. For barrier widths L_L and L_R and well size L_W a linear approximation for the potential profile gives $\alpha = (L_\mathrm{L} + L_\mathrm{W}/2)/(L_\mathrm{L} + L_\mathrm{W} + L_\mathrm{R})$.

3.1. Green's functions and transmittances

To obtain the one-electron transmittances between different channels several methods can be adopted. One possibility is to use the pruning method proposed by Bonča and Trugman and solve for the wave function. An alternative is to work out the Green's functions for the system. The connection between the Green's functions and the scattering matrix was established by Fisher and Lee [31,32] and extended for multilead tight-binding systems by D'Amato and Pastawski [24]. Here we use this last option. First we eliminate the horizontal dangling chains through a decimation procedure [24,33]. We then obtain an effective Hamiltonian for the well site coupled to the phonons:

$$\begin{aligned}\tilde{\mathscr{H}}_{\mathrm{e-ph}} = \sum_{n\geq 0} \{&[E_0 + n\hbar\omega_0 + \Sigma_n(\varepsilon)]|0,n\rangle\langle 0,n| \\ &- \sqrt{n+1}V_\mathrm{g}(|0,n+1\rangle\langle 0,n| + |0,n\rangle \\ &\times\langle 0,n+1|)\},\end{aligned} \tag{5}$$

where the retarded self-energy corrections $\Sigma_n = {}^\mathrm{L}\Sigma_n + {}^\mathrm{R}\Sigma_n$ take into account the electron hopping into the left (L) and right (R) electrodes. These self-energies are given by:

$${}^\mathrm{L}\Sigma_n = \left|\frac{V_\mathrm{L}}{V}\right|^2 \times \Sigma(\varepsilon - n\hbar\omega_0), \tag{6}$$

$${}^\mathrm{R}\Sigma_n = \left|\frac{V_\mathrm{R}}{V}\right|^2 \times \Sigma(\varepsilon - n\hbar\omega_0 + e\mathrm{V}), \tag{7}$$

with

$$\begin{aligned}\Sigma(\varepsilon) &= \Delta(\varepsilon) - \mathrm{i}\Gamma(\varepsilon), \\ \Delta(\varepsilon) &= \frac{1}{\pi}\int \frac{\Gamma(\varepsilon')}{\varepsilon - \varepsilon'}\mathrm{d}\varepsilon',\end{aligned} \tag{8}$$

$$\Gamma(\varepsilon) = \sqrt{V^2 - [(\varepsilon - 2V)/2]^2} \times \theta(\varepsilon) \times \theta(4V - \varepsilon). \tag{9}$$

While the imaginary part $\Gamma = \hbar v_\varepsilon/(2a)$ is proportional to the group velocity v_ε in the electrodes, the actual escape rates $\Gamma_{\mathrm{L(R)}}/\hbar$ are also controlled by the barrier geometry. For width $L_{\mathrm{L(R)}}$ and attenuation length ξ, $\Gamma_{\mathrm{L(R)}}/\Gamma = |V_{\mathrm{L(R)}}/V|^2 \simeq \exp[-L_{\mathrm{L(R)}}/\xi]$.

The retarded Green function connecting states m and n,

$$G^R_{n,m}(\varepsilon) = \langle 0,n|(\varepsilon\mathscr{I} - \tilde{\mathscr{H}}_{\mathrm{e-ph}}(\varepsilon))^{-1}|0,m\rangle \tag{10}$$

has poles at the exact eigen-energies. If $\Sigma_n(\varepsilon) \equiv 0$, these are the polaronic energies $E_0 - (|V_\mathrm{g}|^2/\hbar\omega_0) + n\hbar\omega_0$. The transmission coefficient $T_{n,m}$ from the m-th incoming channel at left electrode to the n-th channel at right is given by [24]:

$$T_{n,m}(\varepsilon) = 2\mathrm{Im}[{}^\mathrm{R}\Sigma_n(\varepsilon)]|G^R_{n,m}(\varepsilon)|^2 2\mathrm{Im}[{}^\mathrm{L}\Sigma_m(\varepsilon)]. \tag{11}$$

In what follows, we will assume a weak electron–phonon coupling, $g = (V_\mathrm{g}/\hbar\omega_0)^2 \ll 1$ (as is the experimental case) and well separated resonances, $(\varepsilon_\mathrm{F}, \Gamma_\mathrm{L} + \Gamma_\mathrm{R}) < \hbar\omega_0$. In the calculation of the currents we will consider the low temperature regime $k_\mathrm{B}\mathrm{T} \ll \varepsilon_F$. Therefore, we will need only the transmittances with zero initial phonons in the system. We consider a Fermi energy $\varepsilon_F \ll V$ as is the case for semiconductors. Then we approximate the self-energy by the following expression:

$$\Sigma(\varepsilon) \approx -\mathrm{i}\Gamma(\varepsilon = \varepsilon_F) \times \theta(\varepsilon). \tag{12}$$

Note that this approximation is different from the usual 'broad-band' approximation [18] since here the Heaviside step function plays a very relevant role by cancelling some transmittances.

The *elastic transmittance*, i.e. without a net phonon emission during the tunneling process, can be obtained from the Green's function:

$$\begin{aligned}G^R_{0,0} \simeq &\frac{1-g}{\varepsilon - \bar{E}_0 + \mathrm{i}[\Gamma_\mathrm{L} + \Gamma_\mathrm{R}]} \\ &+ \frac{g}{\varepsilon - [\bar{E}_0 + \hbar\omega_0] + \mathrm{i}[\tilde{\Gamma}_\mathrm{L} + \Gamma_\mathrm{R}]},\end{aligned} \tag{13}$$

which is evaluated with the first two polaronic states. Here, $\tilde{\Gamma}_\mathrm{L} = g\Gamma_\mathrm{L}$ and $\bar{E}_0 = E_0 - (|V_\mathrm{g}|^2/\hbar\omega_0)$. The first term contains the main resonance associated to the build up of the polaronic ground state and the second term contains a virtual exploration into the first polaronic excitation. It is interesting to note that when $\Gamma \simeq 0$, this Green function would be close to cancellation at an intermediate energy $\bar{E}_0 < \varepsilon < \bar{E}_0 + \hbar\omega_0$ giving rise to an *antiresonance* [33,34]. This concept extends the spectroscopic Fano-resonances [35] to the problem of conductance. Here, this destructive *interference effect* is manifested in a many-body problem (see Ref. [36] for a more detailed discussion). For $g \ll 1$, this effect is less important and, in the whole energy range,

$$T_{0,0} \simeq \frac{4\Gamma_\mathrm{L}\Gamma_\mathrm{R}}{[\varepsilon - \bar{E}_0]^2 + [\Gamma_\mathrm{L} + \Gamma_\mathrm{R}]^2} + \mathscr{O}(g) \tag{14}$$

describes the main resonant elastic peak at $\varepsilon = \bar{E}_0$.

The *inelastic transmittance*, $T_{1,0}$, can be evaluated from:

$$G^R_{1,0} \simeq \frac{-\frac{V_g}{\hbar\omega_0}}{\varepsilon - \bar{E}_0 + i[\Gamma_L + \Gamma_R]} + \frac{\frac{V_g}{\hbar\omega_0}}{\varepsilon - [\bar{E}_0 + \hbar\omega_0] + i[\tilde{\Gamma}_L + \Gamma_R]}, \quad (15)$$

when $\varepsilon + eV > \hbar\omega_0$ escapes are enabled and the poles of this Green's function involve the following processes: a) The first term gives an inelastic component in the transmittance at the main peak. b) The second term provides a satellite peak at $\varepsilon = \bar{E}_0 + \hbar\omega_0$ associated to a polaronic excitation followed by its decay into an escaping electron and a phonon left behind. Since this is the process that interests us, we now restrict ourselves to energies around this satellite peak:

$$T_{1,0} \simeq \frac{4\tilde{\Gamma}_L\Gamma_R}{[\varepsilon - (\bar{E}_0 + \hbar\omega_0)]^2 + [\tilde{\Gamma}_L + \Gamma_R]^2}. \quad (16)$$

This shows that phonon emission is a *resonance in the Fock-space*. A maximal probability ($T_{1,0} = 1$) requires equal rates of formation and decay [34]: $\tilde{\Gamma}_L = \Gamma_R$, which in our RTD implies:

$$L_R \simeq L_L + 2\xi \ln\left[\frac{\hbar\omega_0}{V_g}\right]. \quad (17)$$

Hence, thin barriers with this generalized symmetry condition have $T_{1,0} \simeq 1$ over a broad energy range.

3.2. Inelastic current

Given the transmittances between the different channels, the problem is how to compute the currents. In the Landauer's picture, the view is that of orthogonal scattering states extended along the conductor from the emitter to the collector. This orthogonality implies that the Pauli exclusion principle does not enter in the calculation of the currents. In the presence of inelastic scattering, electrons from different incoming states can occupy the same outgoing state. Thus, if one uses single electron transmittances to represent the many-electrons system, these must be complemented with some factors accounting for the Pauli exclusion [37]. Otherwise, there may be an overflow of the final states. An attempt to solve this problem is the implementation of a self-consistent procedure for the non-equilibrium electron distributions [38]. However, for the *experimental case* of low temperatures ($k_BT \ll \varepsilon_F$) and non-linear response and ($eV - \hbar\omega_o > \varepsilon_F$), there is *no-overflow* in the right lead since electrons with energies up to ε_F do not compete for the same final state. Then, the currents can be computed as in a multilead Landauer picture. The total current from left to right is a sum of the currents through each of the leads on the right corresponding to different number of phonons:

$$I_{tot} = \sum_n I_n. \quad (18)$$

where

$$I_n = \left(\frac{2e}{h}\right)\int_0^{\varepsilon_F} T_{n,0}(\varepsilon)d\varepsilon. \quad (19)$$

Note that inelastic reflection is prevented by the condition $\hbar\omega_0 > \varepsilon_F$.

If we assume perfect interfaces and neglect the momentum transfer between electrons and phonons, the tunneling current for a three-dimensional structure can be obtained in terms of the one-dimensional transmittance. The current that produces the emission of n phonons is obtained from Eq. (19) by integration over the transversal modes:

$$I_n^{3D} = \left(\frac{2e}{h}\right)\int_0^{\varepsilon_F} A\frac{m^*}{2\pi\hbar^2}(\varepsilon_F - \varepsilon)T_{n,0}(\varepsilon)d\varepsilon, \quad (20)$$

where A is the cross-sectional area of the device. The factor that multiplies the transmittance inside the integral takes account of the number of transversal modes with energy between the longitudinal contribution ε to the energy and ε_F. While conservation of transverse electron's momentum might not be fully realistic [29], it constitutes a first approximation yielding results consistent with the main experimental features.

It is interesting to note how the 'decoherence' introduced by the e–ph interaction on the former single particle description can be appreciated. Within this formulation, decoherence arises because the increase in the size of the Hilbert space produces extreme phase fluctuations which prevents the precise prediction of the relative phases of the states required in an interference experiment. Note that even if $\hbar\omega_o \to 0$ the outgoing currents in Eq. (18) cannot interfere. Other points are phase shift fluctuations and the 'broadening' of the resonant energy due to the additional processes of real and virtual phonon emission [36].

From Eq. (19) and the expressions obtained in the previous subsection for the transmittances we will now obtain currents I_0 and I_1. At the satellite peak, the main elastic contribution to the current is provided by the off-resonant tunneling through the ground state, i.e.

$$I_0 \simeq \frac{2e}{h}4\Gamma_L\Gamma_R\varepsilon_F/(\hbar\omega_0)^2. \quad (21)$$

On the other hand, the inelastic current that involves the emission of one phonon in the tunneling process is:

$$I_1 \simeq \frac{e}{\hbar}\frac{4\tilde{\Gamma}_L\Gamma_R}{(\tilde{\Gamma}_L + \Gamma_R)} \times \left[\frac{2}{\pi}\arctan\left(\frac{\varepsilon_F}{2(\tilde{\Gamma}_L + \Gamma_R)}\right)\right]. \quad (22)$$

This current differs from that resulting from the use of rate equations [16] by the factor in brackets which is

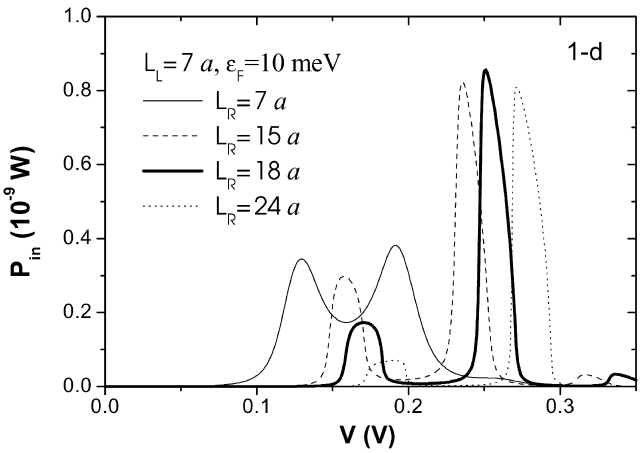

Fig. 3. Power emitted as LO phonons as a function of the applied voltage in one-dimension for $L_L = 7a$ (19.7 Å) and different values of L_R. In this figure, the Fermi energy is taken equal to 10 meV.

fundamental to resolve extreme regimes:

$$I_1 \simeq \begin{cases} \dfrac{e}{h} 4\tilde{\Gamma}_L \Gamma_R/(\tilde{\Gamma}_L + \Gamma_R), & \text{for } \varepsilon_F \gg (\tilde{\Gamma}_L + \Gamma_R), \\ \dfrac{2e}{h} T_{1,0}(\bar{E}_0 + \hbar\omega_0) \times \varepsilon_F, & \text{for } \varepsilon_F \ll (\tilde{\Gamma}_L + \Gamma_R). \end{cases} \quad (23)$$

When $\varepsilon_F \gg (\tilde{\Gamma}_L + \Gamma_R)$ the inelastic current becomes independent of the right barrier geometry in the wide range of geometries where $\varepsilon_F \gg \Gamma_R > \tilde{\Gamma}_L$. In the opposite case I_1, and hence the power emitted as phonons $I_1\hbar\omega_0/e$, becomes determined by the transmittance at resonance, which is maximized by the generalized symmetry condition of Eq. (17).

3.3. Efficiency of the phonon emission

In a general situation where we allow the emission of n phonons, the quantity of interest to analyze the optimization of the phonon emission in the device is the power emitted. The power associated with current I_0 degrades fully into inconvenient electrode heating, while the other terms ($n > 0$) have an important contribution as useful phonon modes. The power emitted as LO phonons is related to the inelastic components of the current:

$$P_{in} = \hbar\omega_0 \sum_{n>0} n \frac{I_n}{e}. \quad (24)$$

The efficiency of the device to transform the electric potential energy into LO-phonon energy can be characterized by the ratio, η, between P_{in} and the total power P dissipated by the electrons

$$\eta = \frac{P_{in}}{P} = \frac{P_{in}}{I_{tot}V}. \quad (25)$$

Using Eq. (24), this expression can be written as:

$$\eta = \frac{\hbar\omega_0 \sum_{n>0} n \dfrac{I_n}{e}}{I_{tot}V}.$$

Each current term, $I_n (n > 0)$, contributes with n useful phonons, while the energy associated with I_0 degrades fully into electrode heating. Then, one might seek a maximal ratio between the inelastic power P_{in} and the total power P. As a function of the applied voltage the efficiency is expected to have a maximum at the voltage corresponding to the satellite peak. At the voltage tuning the resonance at the satellite peak $V_0 \simeq (E_{(o)} - |V_g|^2/\hbar\omega_0 + \hbar\omega_0 - \varepsilon_F/2)/\alpha$, the lowest order of η can be written from Eqs. (21) and (22) as:

$$\eta \simeq \frac{\hbar\omega_0}{eV_0}\left[\frac{I_1}{(I_0 + I_1)}\right]. \quad (26)$$

The factor in brackets is small for narrow barriers because non-resonant tunneling dominates over phonon-assisted tunneling, thus reducing the inelastic current as compared to the elastic component. For wide barriers, this factor goes to one as $\tilde{\Gamma}_L + \Gamma_R \to 0$. The other factor decreases with increasing right barrier's width because it requires a higher V_0. Thus, as Γ_R is decreased, two effects compete: the switch from non-resonant to phonon assisted resonant tunneling and an excess in the electronic kinetic energy in the collector. Hence, as long as the left barrier is not extremely thin ($\Gamma_L > \hbar\omega_0$), η cannot depend much on geometry. With this restriction in mind, a device designed for phonon production should maximize the emitted power according to Eq. (17).

4. Numerical results

In this section we will contrast the previous predictions

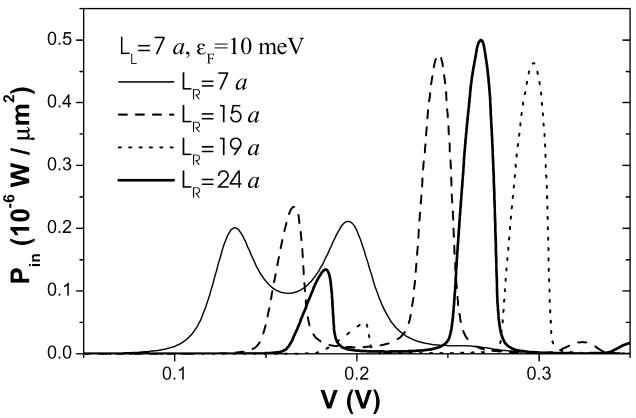

Fig. 4. Same as Fig. 2 but in three-dimensions.

with the numerical results of a description involving geometry, voltage and energy dependences of a typical RTD. We consider the Hamiltonian of Eqs. (1–4).

In what follows, we consider the low temperature limit in which there are no phonons before the scattering process. The parameters in our calculations are chosen to simulate the case of a GaAs-AlGaAs structure. The effective mass m^* is taken to be $0.067m_e$, the LO phonon frequency $\hbar\omega_0 = 36$ meV, the discretization constant used in our calculations is $a = 2.825$ Å and the value of the hopping parameter $V = 7.125$ eV. The electron–LO-phonon coupling constant V_g is taken to be 10 meV which gives a typical electron–phonon interaction strength $g = (V_g/\hbar\omega_0)^2 \sim 0.1$. The barrier heights are 300 meV and the Fermi energy ε_F is taken equal to 10 and 20 meV. We consider a well of 56.5 Å (corresponding to 20 layers of GaAs grown in the [100] direction). N_L, N_R and N_W are the number of sites in the left and right barriers and the well, the associated widths are $L_i = N_i a$. Up to $N_{ph} = 3$ phonon quanta are considered in the calculations. This gives satisfactory accuracy in the whole range of energy.

4.1. Power emitted as LO-phonons

Let us consider the case of a *thin left barrier* (with a typical transmission probability $T_L(\varepsilon_F) = \Gamma_L/\Gamma \sim 0.03$). In Fig. 3 we show $P_{in}-V$ curves in one-dimension calculated according to Eq. (19) for various right barrier widths L_R. We observe two main peaks, a) and b), which are separated approximately by

$$\delta V \simeq \frac{\hbar\omega_0}{\alpha e},$$

where αeV is the typical energy gain from the electric field at the time of phonon emission. In a linear approximation

$$\alpha = \frac{L_L + L_W/2}{L_L + L_W + L_R}.$$

We are interested in the optimization of the emission of LO phonons at the second peak. This allows for the highest efficiency factor while keeping an appreciable phonon emission.

Fig. 3 shows that the peaks are shifted to higher voltages as L_R is increased. This reflects a strong renormalization of

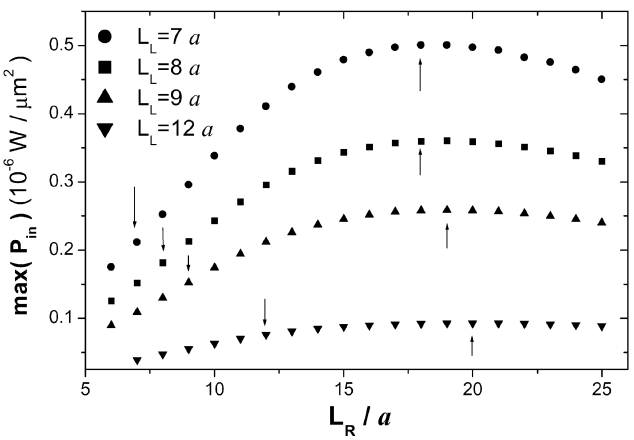

Fig. 5. Maximum value of the power emitted as LO phonons for different barrier geometries (in 3-d) and $\varepsilon_F = 10$ meV. The symmetric situations are marked with a downward arrow and the situations of optimized phonon emission are marked with an upward arrow.

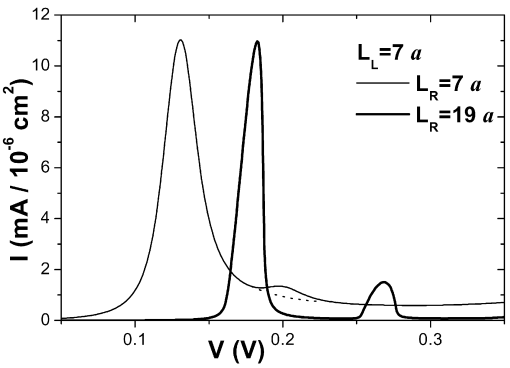

Fig. 6. Current density as a function of the applied voltage for a symmetrical (thin line) structure and the optimized structure. These results correspond to $L_{\rm L} = 7a$ (19.7 Å) and $\varepsilon_F = 10$ meV in three-dimensions.

the resonant energies due to the asymmetry of the barriers. We can understand this by noting that when a potential eV is applied to the double barrier, the resonant energies are lowered approximately by a factor αeV. Thus, for wider right barriers the resonant energies are shifted to higher values.

We can also see that the peak value of $P_{\rm in}$, max($P_{\rm in}$), exhibits a maximum as a function of the right barrier width. This behavior is also present in the curve for $P_{\rm in}$ as a function of the voltage V in three-dimensions calculated according to Eq. (20) as can be appreciated in Fig. 4.

In Fig. 5 we present max($P_{\rm in}$) versus $L_{\rm R}$ curves for $L_{\rm L} = 7a, 8a, 9a, 12a$ in three-dimensions, which correspond to emitter lengths between 20 and 25 Å. These curves exhibit a maximum for max($P_{\rm in}$) as a function of $L_{\rm R}$. The optimal configurations correspond to asymmetric structures with right barriers which are about twice of the left ones. Notice also that the curves are shifted to lower power values when

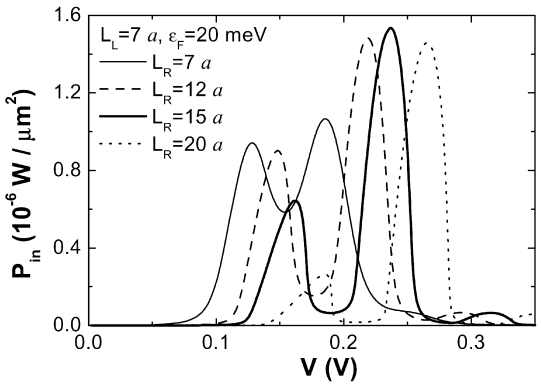

Fig. 7. Power emitted as LO phonons as a function of the applied voltage in three-dimensions for $L_{\rm L} = 7a$ (19.7 Å) and different values of $L_{\rm R}$. In this figure, the Fermi energy is taken equal to 20 meV.

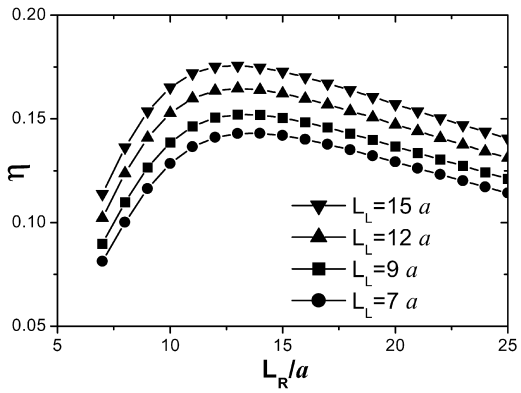

Fig. 8. Efficiency of the device to emit LO phonons as a function of the right barrier width for various left barrier geometries in 3-d and $\varepsilon_F = 10$ meV.

the left barrier width is increased. This is due to a corresponding increase in the reflectivity of the device.

These results confirm that, for a given $L_{\rm L}$ satisfying $\Gamma_{\rm L} < \hbar\omega_0$ and $g\Gamma_{\rm L} + \Gamma_{\rm R} > \varepsilon_F$, the phonon emission rate is enhanced (by a factor 2.5 in the case of Fig. 3) by choosing a wider right barrier as prescribed by Eq. (17). This explains the unusually large satellite peaks of asymmetric structures [29]. In Fig. 6 the I–V curves for the symmetric and the optimal asymmetric RTDs are shown.

Let us consider RTD's where these conditions ($\Gamma_{\rm L} < \hbar\omega_0$ and $g\Gamma_{\rm L} + \Gamma_{\rm R} > \varepsilon_F$) are relaxed. One possibility is to use wider left barriers. In Fig. 5 we see that the trend is to flatten the optimum as we go to wider left barriers. Hence, consistently with our discussion in Section 2, there is no substantial gain in $P_{\rm in}$ by choosing an asymmetric structure in these cases. Another possibility is to increase the Fermi energy. In Fig. 7 we show $P_{\rm in}$–V curves in three-dimensions for various right barrier widths $L_{\rm R}$ for $\varepsilon_F = 20$ meV. Comparison with Fig. 4, which corresponds to $\varepsilon_F = 10$ meV, shows that the optimal geometry is less asymmetric and that the optimization of the phonon emission is weaker: a factor 2.5 versus a factor 1.4 in Fig. 7. This is also consistent with the behavior expected from the analytical results.

4.2. Efficiency

In Fig. 8 we show the efficiency η, evaluated at the optimal voltage, as a function of the right barrier width for various $L_{\rm L}$ where $\Gamma_{\rm L} < \hbar\omega_0$. In agreement with our theoretical analysis, η keeps the same magnitude for all the geometrical configurations shown in the figure.

Note also in Fig. 8 that devices with wide barriers have efficiencies which are of the same order as those corresponding to more transparent ones. However, the power emitted as LO phonons in the quasi-transparent barriers surpasses that of the opaque ones in two orders of

magnitude. As a consequence, in order to obtain a high emission of primary phonons, it would be advantageous to construct a device with narrow asymmetric barriers as in the optimum situations in Fig. 4.

5. Conclusions

In summary, we have proposed an alternative RTD-based ultrasound emitter (SASER). We have analyzed in detail the optimization of the geometrical parameters of the RTD to maximize the emission of LO phonons. We have shown, both analytically and numerically, that an appropriate geometry of the barriers can substantially enhance the phonon emission. In particular, we have shown that for thin left barriers (of about 28 Å for AlGaAs), the optimal configurations correspond to collector barriers whose widths are about twice that of the emitter. In contrast, for devices with wide barriers (of about 68 Å for AlGaAs) the power emitted as LO phonons is sensibly reduced and no appreciable geometrical optimization is found. The validity of the model employed requires a restriction of the decay into many vibrational modes which could be achieved by $\varepsilon_F \ll \hbar\omega_0$, or even better by frozen the transversal degrees of freedom by applying a strong magnetic field [6,7] or by lateral confinement.

Although we used parametrizations that describe the especific case of electron–phonon interaction in standard RTD geometries, the essence of our analysis only involves the optimation of an inelastic resonance for electronic tunneling where each electronic state interacts with an elementary excitation. This is a totally general result, independent of the details of the model adopted and hence the line of reasoning could also be applied to many other problems regardless of whether the excitations are of optical, magnetic or vibrational nature [9].

Acknowledgements

We acknowledge financial support from CONICET, SeCyT-UNC, ANPCyT and Andes-Vitae-Antorchas. H.M.P. and L.E.F.F.T. benefited from discussions with Yu. M. Galperin and the hospitality of ICTP (Trieste).

References

[1] L.P. Kouwenhoven, et al., in: L.L. Sohn, L.P. Kouwenhoven, G. Schön, (Eds.), Mesoscopic Electron Transport, Kluwer Academic Publishers, Dordrecht, 1997.
[2] J.K.G.C. Joachim, A. Aviram, Nature 408 (2000) 541.
[3] R. Landauer, Phys. Lett. 85A (1981) 91.
[4] M. Büttiker, Phys. Rev. Lett. 57 (1986) 1761.
[5] V.J. Goldman, D.C. Tsui, J.E. Cunningham, Phys. Rev. B 36 (1987) 7635.
[6] M.L. Leadbeater, E.S. Eaves, M. Henini, et al., Phys. Rev. B 39 (1989) 3438.
[7] G.S. Boebinger, A.F.J. Levi, S. Schmitt-Rink, et al., Phys. Rev. Lett. 65 (1990) 235.
[8] L.P. Kouwenhoven, Nature 407 (2000) 35.
[9] H. Park, J. Park, A.K.L. Kim, et al., Nature 407 (2000) 57.
[10] B.C. Stipe, M.A. Rezaei, W. Ho, Phys. Rev. Lett. 81 (1998) 1263.
[11] F. Vallée, Phys. Rev. B 49 (1994) 2460.
[12] E.V. Anda, S.S. Makler, H.M. Pastawski, R.G. Barrera, Braz. J. Phys. 24 (1994) 330.
[13] S.S. Makler, M.I. Vasilevskiy, E.V. Anda, D.E. Tuyarot, J. Weberszpil, H.M. Pastawski, J. Phys. Condens. Matter 10 (1998) 5905.
[14] I. Camps, S.S. Makler, Solid State Commun. 116 (2000) 191.
[15] S.S. Makler, I. Camps, S. Weberszpil, D. Tuyarot, J. Phys.: Condens. Matter 12 (2000) 3149.
[16] R.G. Lake, G. Klimeck, M.P. Anantram, S. Datta, Phys. Rev. B 48 (1993) 15132.
[17] Foa Torres, L.E.F., Pastawski, H.M., Makler, S.S., 2000. Physica A 283, 297; Phys. Rev. B 64 (2001) 193304.
[18] N.S. Wingreen, K.W. Jacobsen, J.W. Wilkins, Phys. Rev. Lett. 61 (1988) 1396.
[19] N.S. Wingreen, K.W. Jacobsen, J.W. Wilkins, Phys. Rev. B 40 (1989) 11834.
[20] L.I. Glazman, R.I. Shekter, Zh. Eksp. Teor. Fiz. 94 (1988) 292 [Sov. Phys. JETP 67 (1988) 163].
[21] J.A. Støvneng, E.H. Hauge, J.A. Lipavský, J.A. Spička, Phys. Rev. B 44 (1991) 13595.
[22] N. Zou, K.A. Chao, Phys. Rev. Lett. 69 (1992) 3224.
[23] N. Zou, K.A. Chao, Yu.M. Galperin, Phys. Rev. Lett. 71 (1993) 1756.
[24] J.L. D'Amato, H.M. Pastawski, Phys. Rev. B 41 (1990) 7411.
[25] S. Datta, Phys. Rev. B 40 (1989) 5830.
[26] L.V. Keldysh, Zh. Eksp. Teor. Fiz. 91 (1986) 1815 [Sov. Phys. JETP 64 (1986) 1075].
[27] H.M. Pastawski, Phys. Rev. B 46 (1992) 4053.
[28] G.K.R. Lake, R.C. Bowen, D. Jovanovic, J. Appl. Phys. 81 (1997) 7845.
[29] P.J. Turley, C.R. Wallis, S.W. Teitsworth, W. Li, P.K. Bhattacharya, Phys. Rev. B 47 (1993) 12640.
[30] J. Bonča, S.A. Trugman, Phys. Rev. Lett. 75 (1995) 2566.
[31] D.S. Fisher, P.A. Lee, Phys. Rev. B 23 (1981) 6851.
[32] H.M. Pastawski, E. Medina, Rev. Mex. Fis. 47 Suppl. 1 (2001) 1 also available at cond-mat/0103219.
[33] P.R. Levstein, H.M. Pastawski, J.L. D'Amato, J. Phys.: Condens. Matter 2 (1990) 1781.
[34] J.L. D'Amato, H.M. Pastawski, J.F. Weisz, Phys. Rev. B 39 (1989) 3554.
[35] U. Fano, Phys. Rev. 124 (1961) 1866.
[36] Pastawski, H.M., Foa Torres, L.E.F., Medina, E. Chem. Phys. 281, (2002) 257.
[37] M. Wagner, Phys. Rev. Lett. 85 (2000) 174.
[38] E.G. Emberly, G. Kirczenow, Phys. Rev. B 61 (2000) 5740.